Electronic Supplementary Material (ESI) for Lab on a Chip.

Title:

Scaling and Automation of High-Throughput Single-Cell-Derived Tumor Sphere Assay Chip

Authors and affiliations:

Yu-Heng Cheng[a], Yu-Chih Chen[a, b], Riley Brien[a], and Euisik Yoon*[a, c]

[a]Department of Electrical Engineering and Computer Science, University of Michigan, 1301 Beal Avenue, Ann Arbor, MI 48109-2122;

[b]University of Michigan Comprehensive Cancer Center, 1500 E. Medical Center Drive, Ann Arbor, MI 48109, USA

[c] Department of Biomedical Engineering, University of Michigan, 2200 Bonisteel, Blvd. Ann Arbor, MI 48109-2099, USA

*Corresponding author

Yu-Heng Cheng
1301 Beal Avenue, Ann Arbor, MI 48109-2122, USA
Tel: 734-353-5391; E-mail: yhcheng@umich.edu.

Euisik Yoon
1301 Beal Avenue, Ann Arbor, MI 48109-2122, USA
Tel: 734-615-4469; E-mail: esyoon@umich.edu.

Supplementary Figures

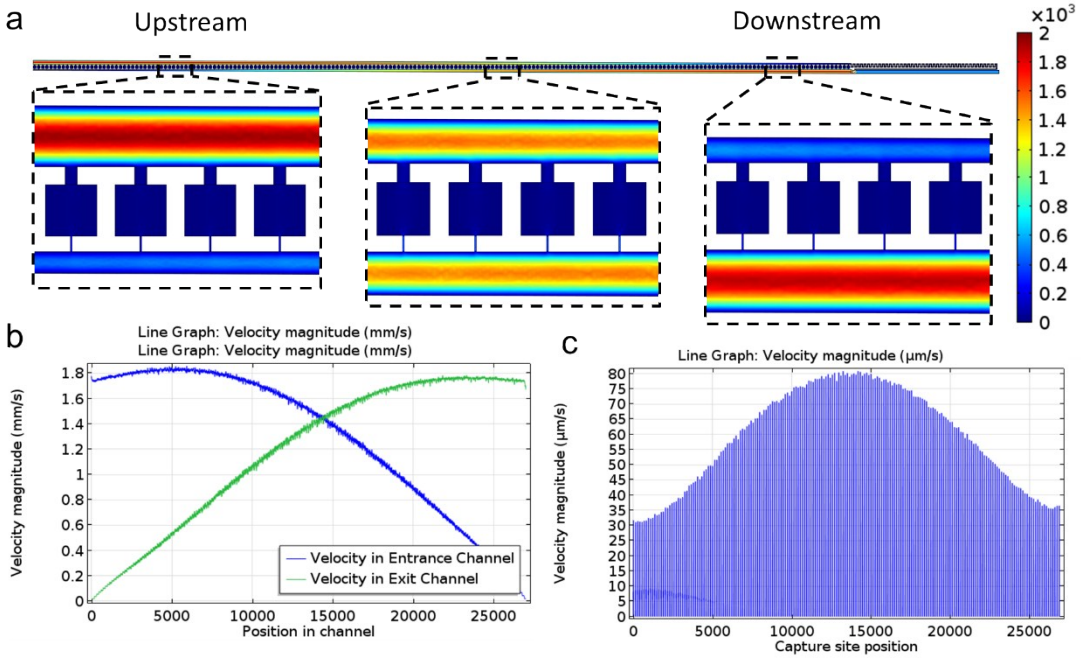

Figure S1. (a) Simulation of one branch channel with 50 Pa input pressure (unit: μm/min) (b) The tapered entrance and exit channel help maintain the constant flow rate at the upstream and midstream (c) Flow distribution across the 200 capture sites, showing higher flow rate at the midstream and lower flow rate at the upstream and downstream with ~65% difference from peak value. Although this distribution can be more uniform (<10% difference) by making the averaged cross-section of entrance channel larger, i.e. 150×200 μm instead of 85×100μm, this design is sufficient for robust single cell capture.

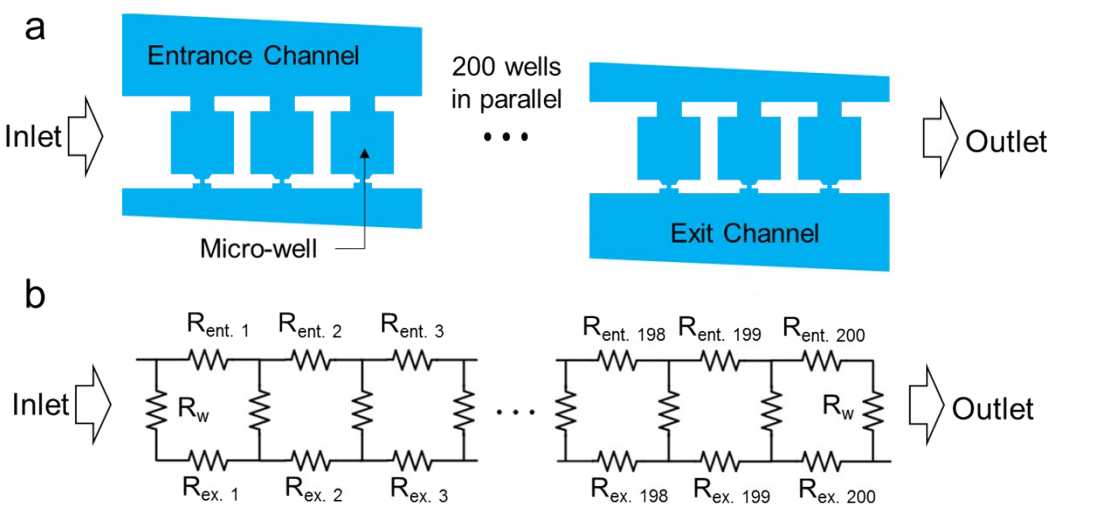

Figure S2. Fluidic circuit analogy for channel design. (a) Channel diagram of a single branch channel. (b) Equivalent electrical circuit diagram to the fluidic channel in (a). $R_{ent.}$ *is the unit resistance of an entrance channel segment between two neighboring wells. The resistance gradually increases from* $R_{ent.\ 1}$ *to* $R_{ent.\ 200}$ *due to the tapered channel.* R_w *is the resistance through each micro-well.* $R_{ex.}$ *is the unit resistance of an exit channel segment between two neighboring wells. The resistance gradually decreases from* $R_{ex.\ 1}$ *to* $R_{ex.\ 200}$ *due to the tapered channel.*

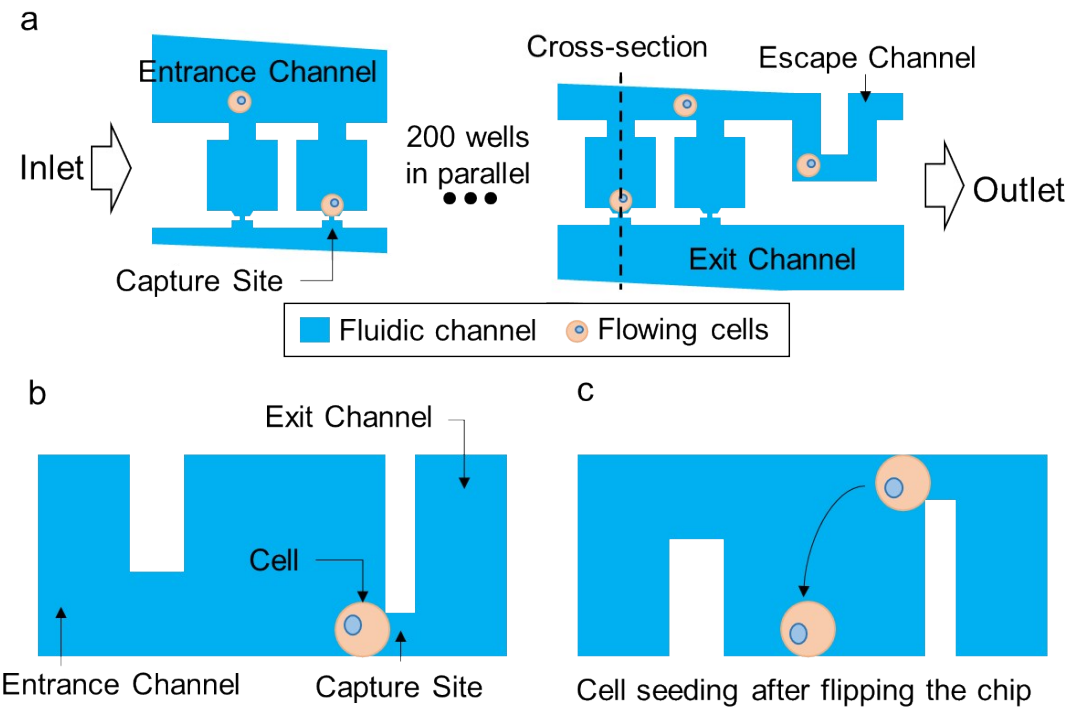

Figure S3. Cross-section diagram showing cell seeding after capture. (a) Overview of the fluidic channel with cells captured at capture sites. (b) A cross-section view of a captured cell from (a). (c) After flipping the chip, cells are seeded into each individual well by gravity for sphere culture.

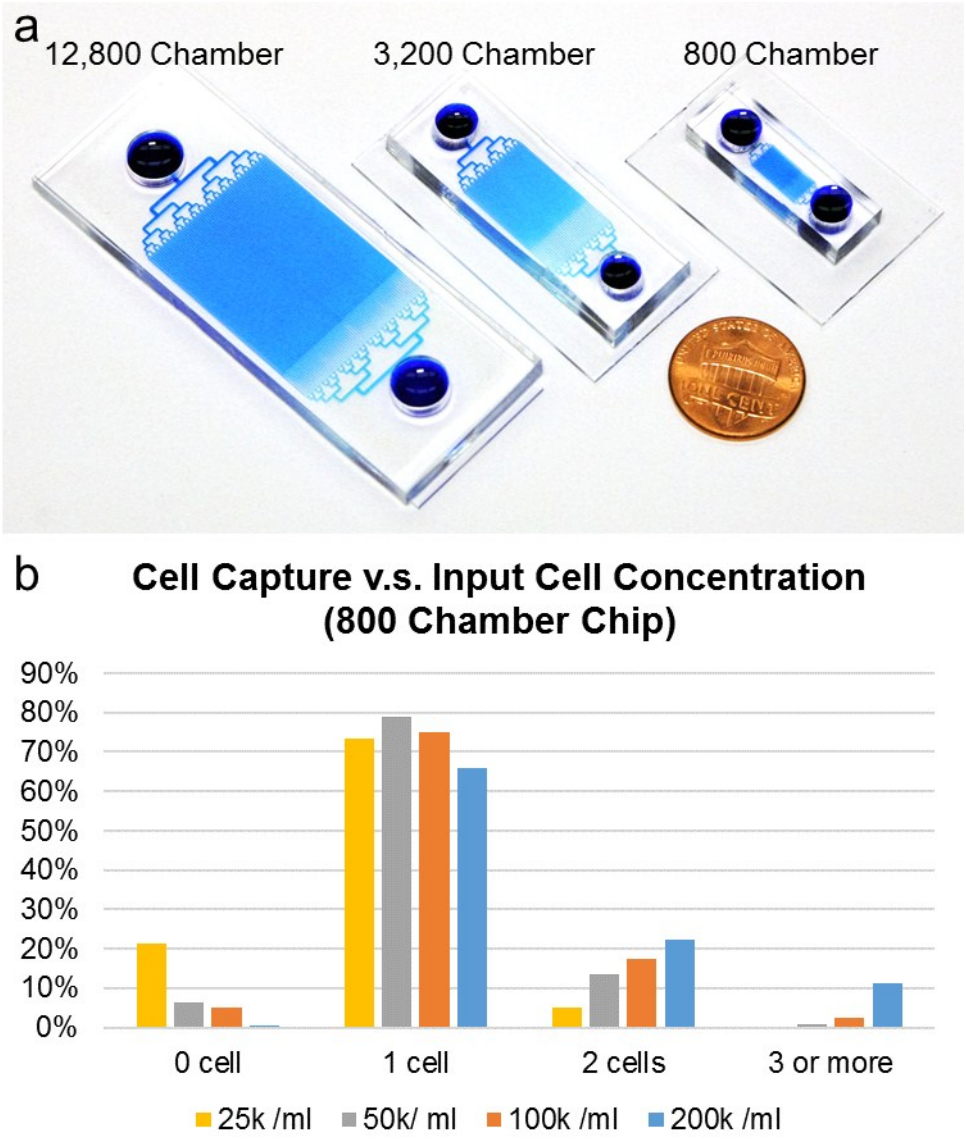

Figure S4. (a) Picture of devices with 800 chambers, 3,200 chambers, and 12,800 chambers for single cell capture and culture (b) Cell capture distribution for the 800 chamber chip, showing similar capture distribution compared to the 12,800 chamber chip. (N=1 for each concentration)

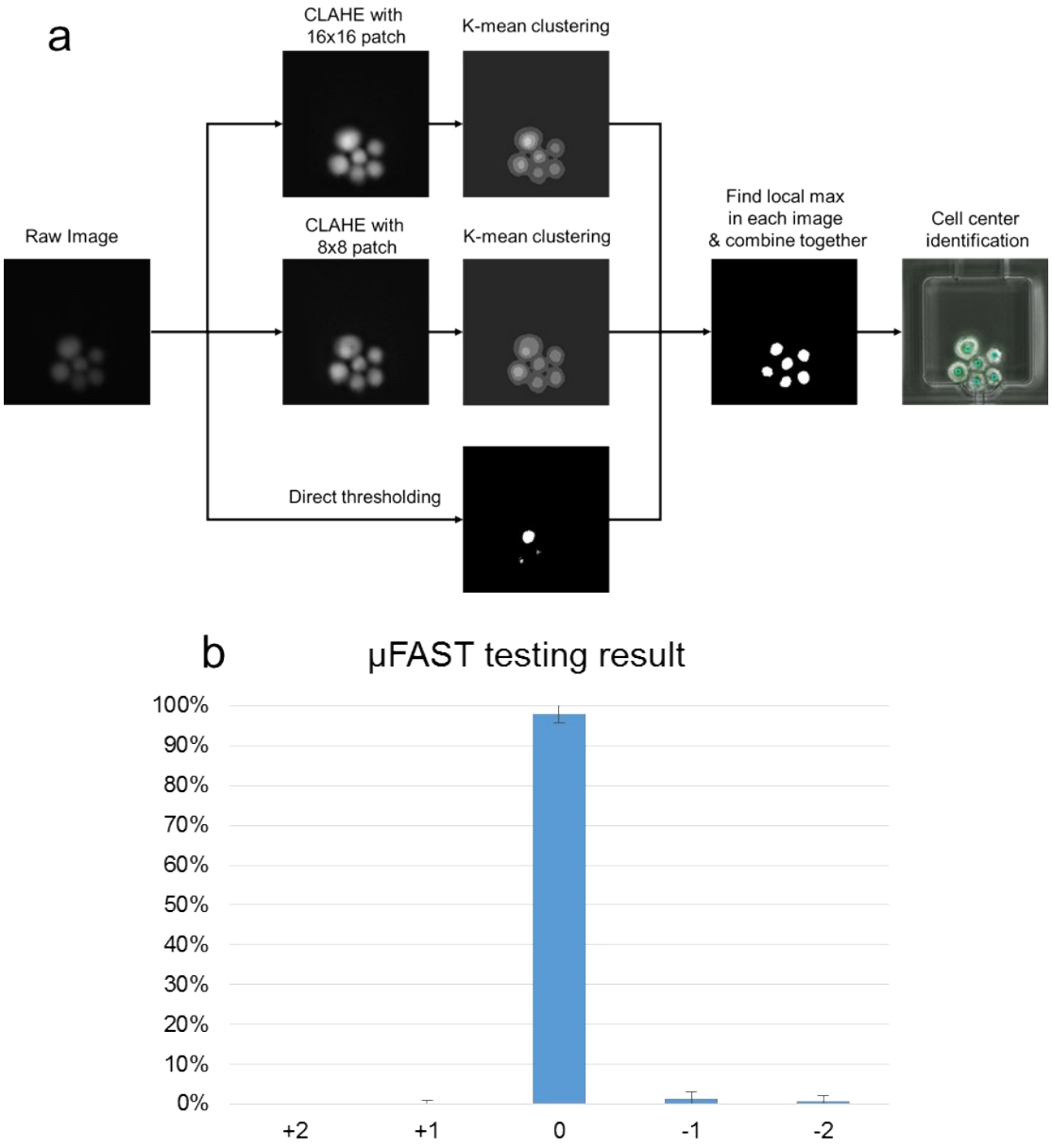

Figure S5. µFAST cell counting working flow and accuracy testing result (a) Step-by-step diagram of cell counting. (b) Example of accuracy testing result, showing 98% high accuracy with few cases of over-count (+1 and +2) and under-count (-1 and -2). (N=6 with total 350 micro-wells tested)

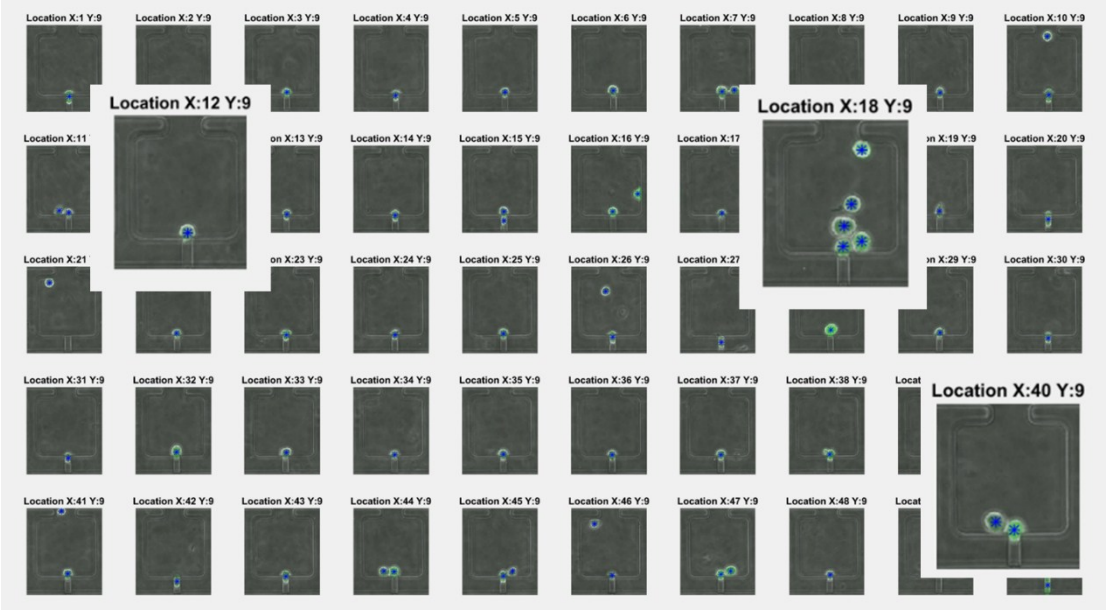

Figure S6. An example of cell counting panel after cell capture to confirm counting accuracy. Location X:12 Y:9 shows the single cell counting. Location X:40 Y:9 shows the case with two cells attaching to each other. Location X:18 Y:9 shows multiple cells counting.

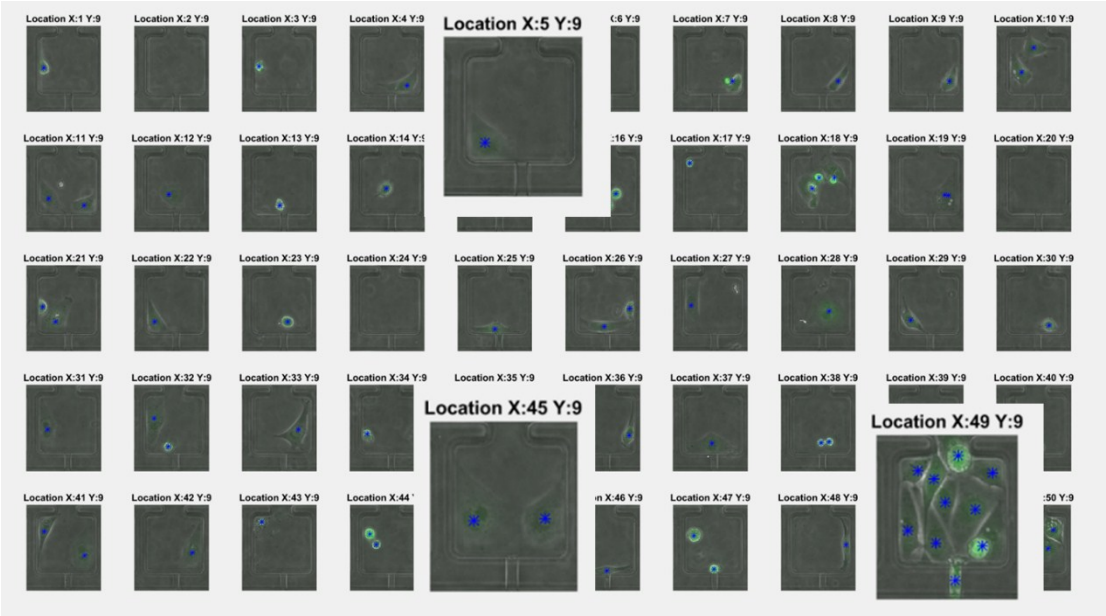

Figure S7. An example of cell counting panel for adherent culture. Location X:6 Y:9 shows single cell counting; Location X:6 Y:9 shows counting of two adherent cells; Location X:49 Y:9 shows cell counting of a confluent well, validating the counting accuracy of uFAST.

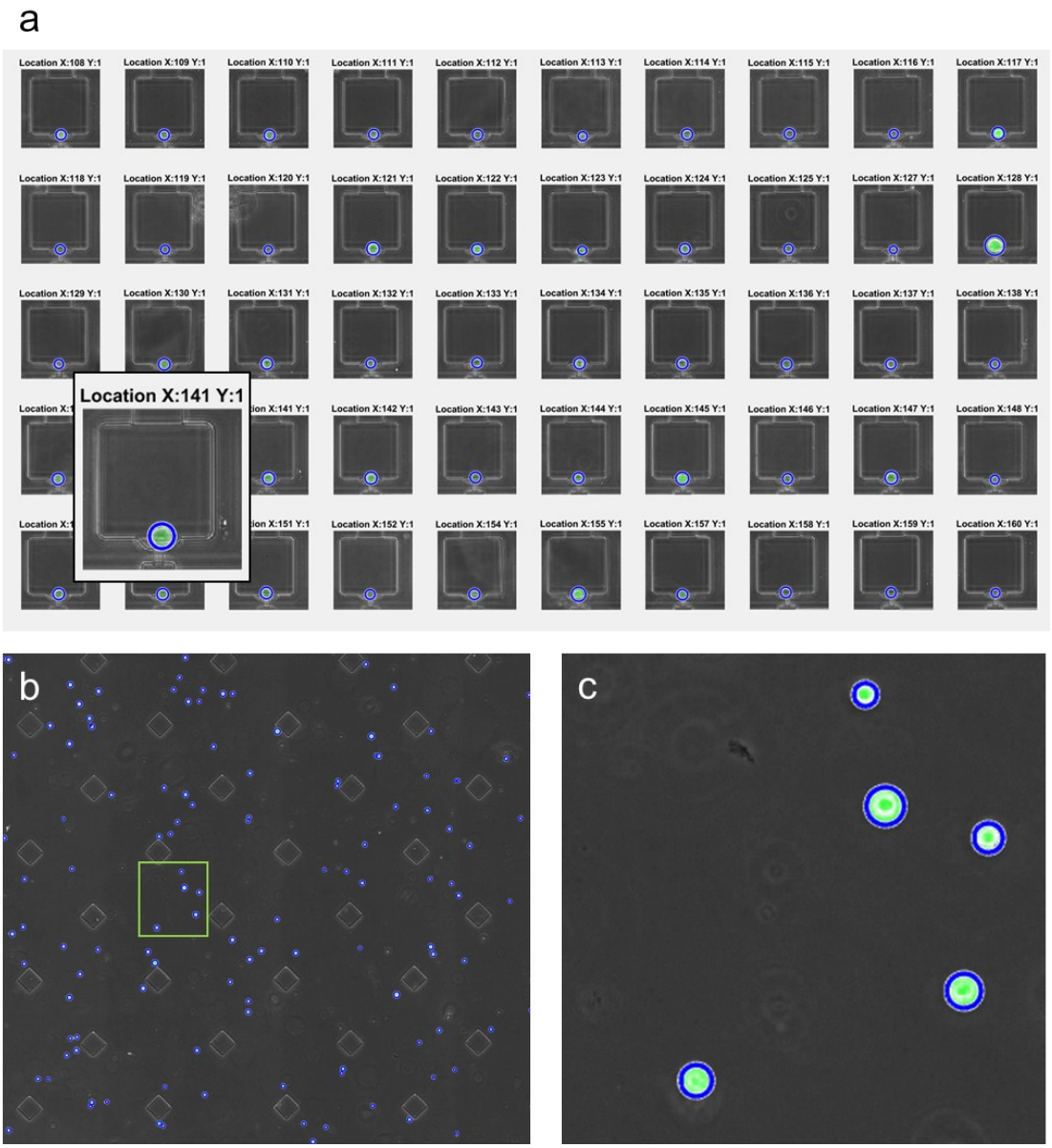

Figure S8. Cell size measurement with each cell size highlighted in blue circle. (a) An example of cell size measurement panel for cells captured on chip. (b) To measure bulk cell size distribution, cells were flooded into a 100μm-high chamber to ensure good imaging quality with cells on the same focal plane. (c) Cell size measurement of cells in bulk from the yellow box in (b).

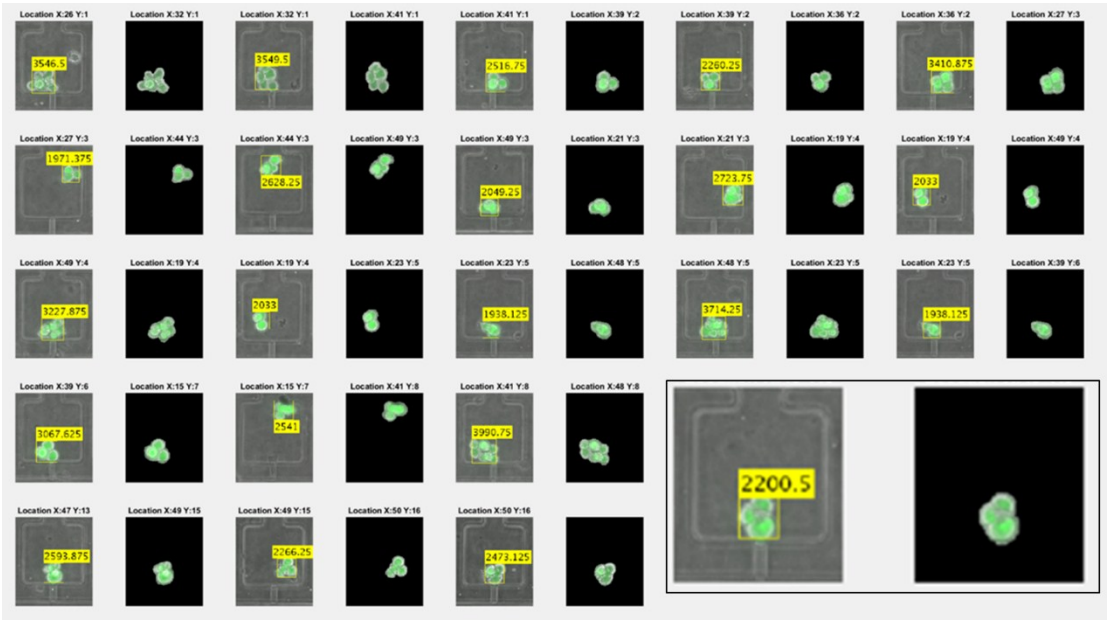

Figure S9. Sphere size measurement by fluorescent intensity thresholding

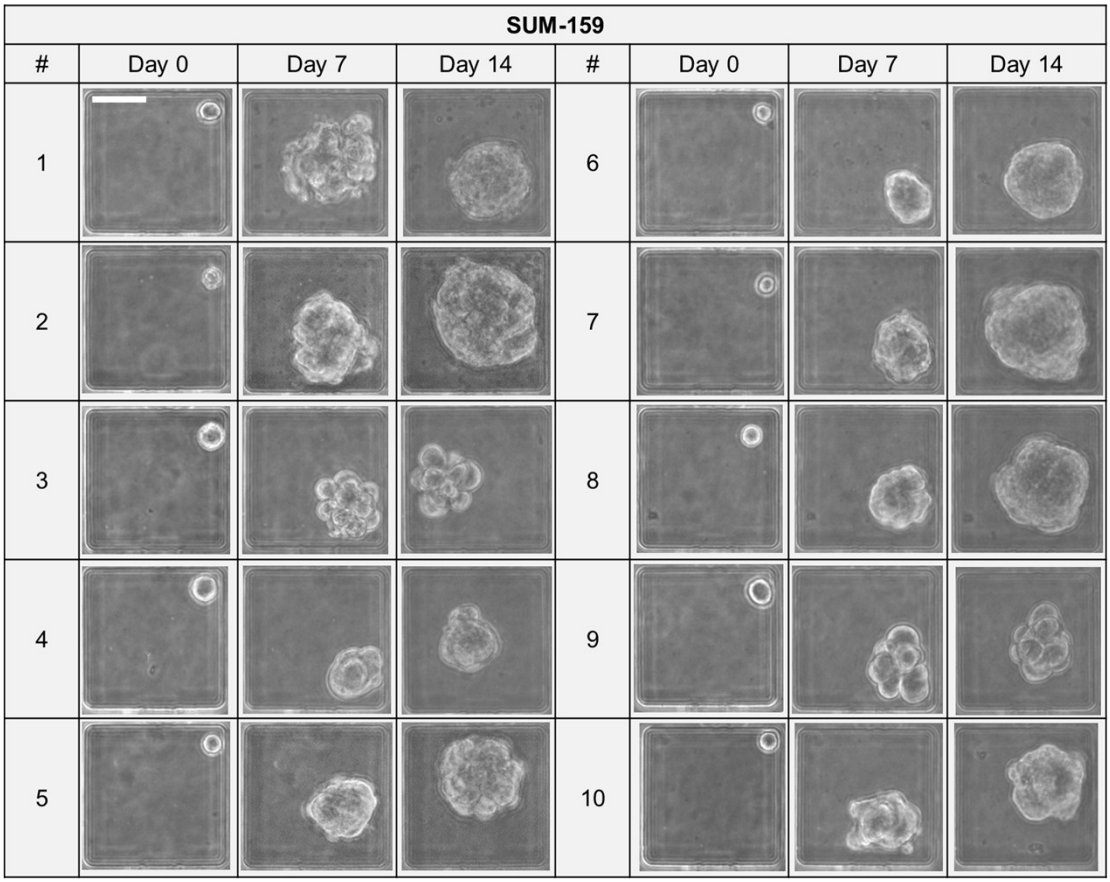

Figure S10. Microscopic images of SUM-159 single-cell-derived spheres (Scale bar: 40μm)

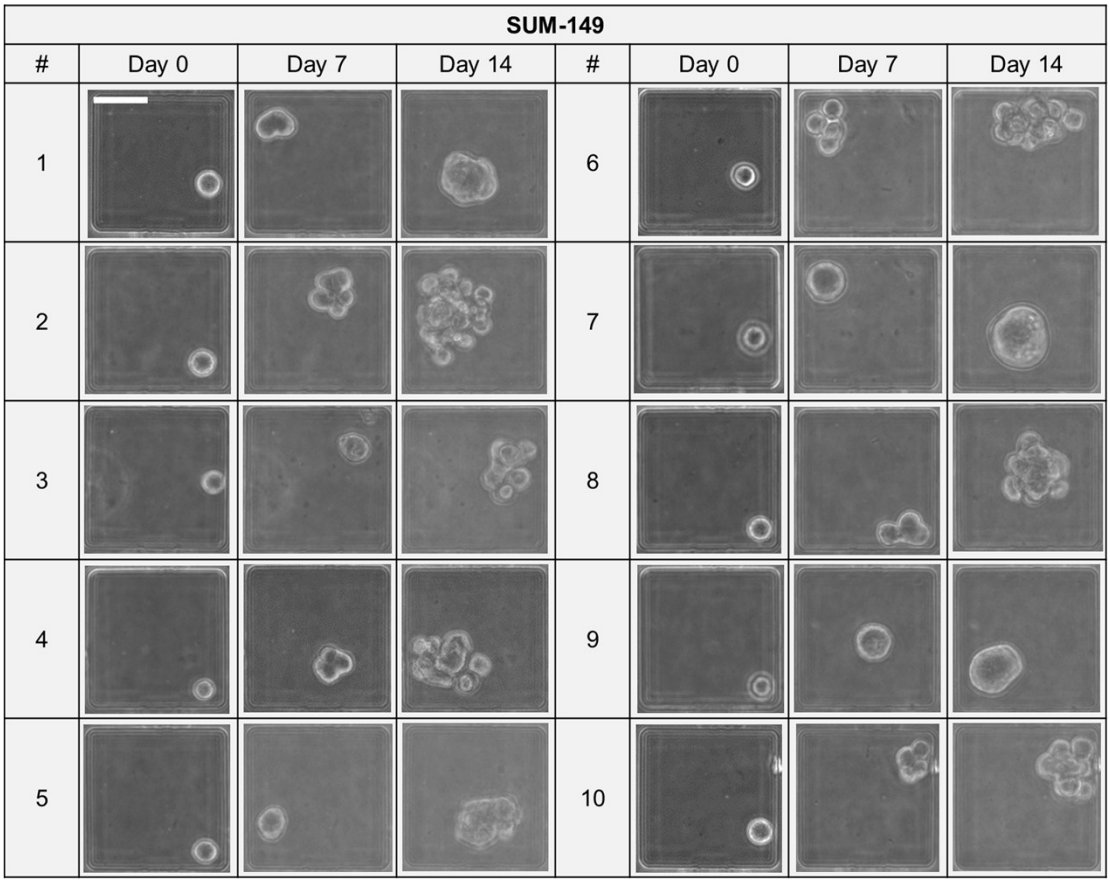

Figure S11. Microscopic images of SUM-149 single-cell-derived spheres. (Scale bar: 40μm)

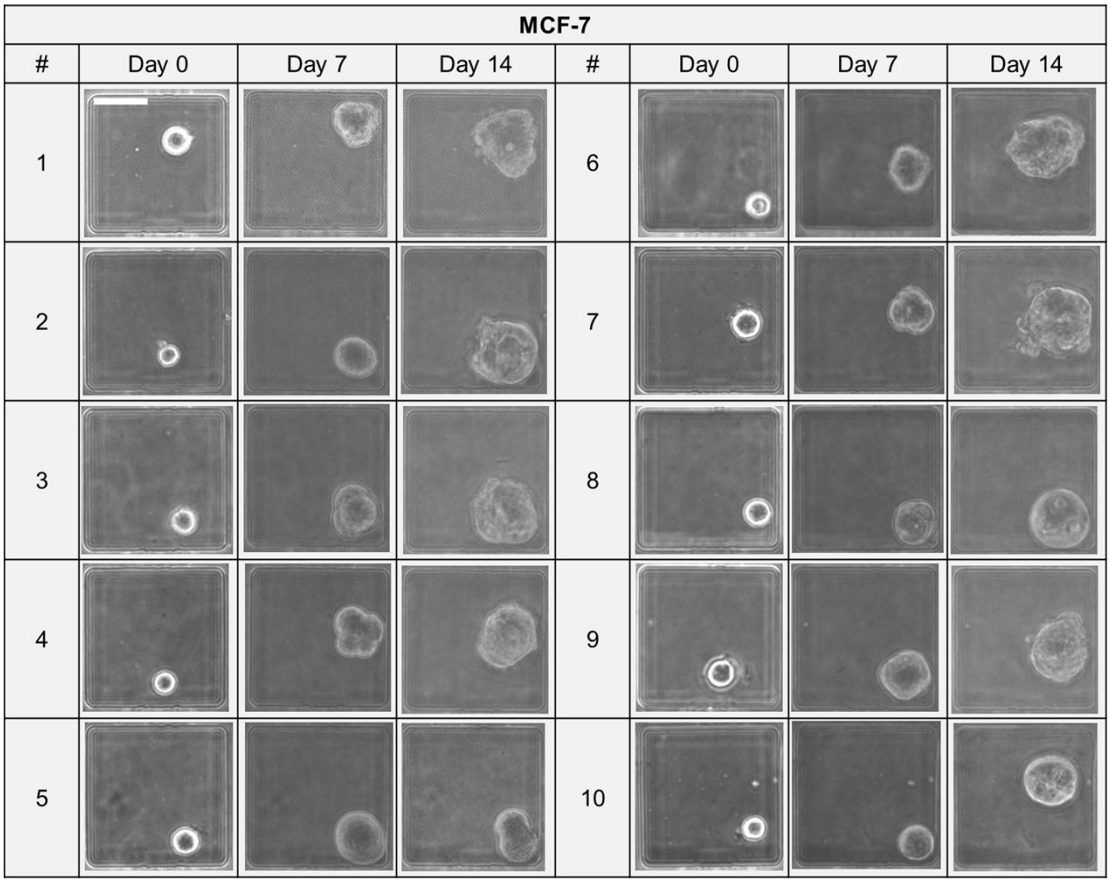

Figure S12. Microscopic images of MCF-7 single-cell-derived spheres. (Scale bar: 40μm)

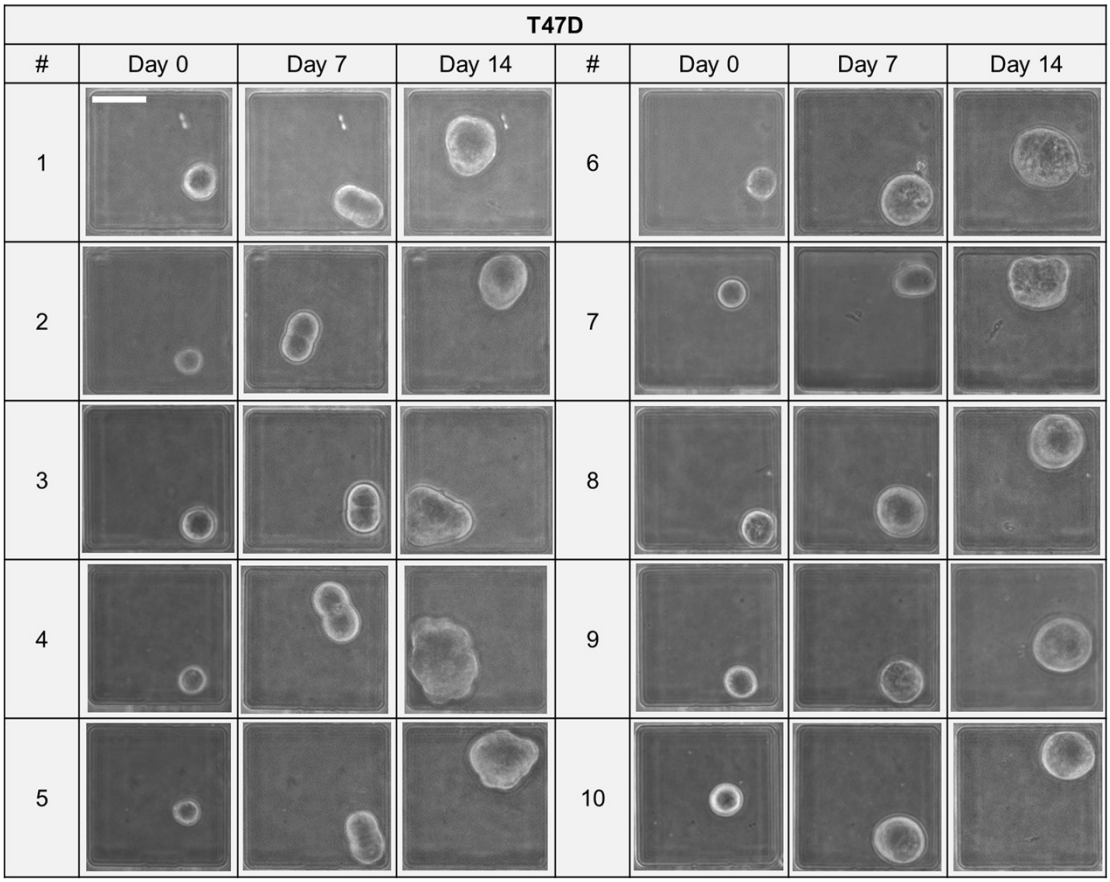

Figure S13. Microscopic images of T47D single-cell-derived spheres. (Scale bar: 40μm)